

Dual-level Mixup for Graph Few-shot Learning with Fewer Tasks

Yonghao Liu*
Mengyu Li*
College of Computer Science and
Technology, Jilin University
Changchun, China
yonghao20@mails.jlu.edu.cn
mengyul21@mails.jlu.edu.cn

Fausto Giunchiglia
Department of Information
Engineering and Computer Science,
University of Trento
Trento, Italy
fausto.giunchiglia@unitn.it

Lan Huang*
College of Computer Science and
Technology, Jilin University
Changchun, China
huanglan@jlu.edu.cn

Ximing Li*
College of Computer Science and
Technology, Jilin University
Changchun, China
liximing86@gmail.com

Xiaoyue Feng*[†]
College of Computer Science and
Technology, Jilin University
Changchun, China
fengxy@jlu.edu.cn

Renchu Guan*[†]
College of Computer Science and
Technology, Jilin University
Changchun, China
guanrenchu@jlu.edu.cn

Abstract

Graph neural networks have been demonstrated as a powerful paradigm for effectively learning graph-structured data on the *web* and mining content from it. Current leading graph models require a large number of labeled samples for training, which unavoidably leads to overfitting in few-shot scenarios. Recent research has sought to alleviate this issue by simultaneously leveraging graph learning and meta-learning paradigms. However, these graph meta-learning models assume the availability of numerous meta-training tasks to learn transferable meta-knowledge. Such assumption may not be feasible in the real world due to the difficulty of constructing tasks and the substantial costs involved. Therefore, we propose a **Si**Mple yet **eff**ective approach for graph few-shot Learning with **f**ewer tasks, named **SMILE**. We introduce a dual-level mixup strategy, encompassing both within-task and across-task mixup, to simultaneously enrich the available nodes and tasks in meta-learning. Moreover, we explicitly leverage the prior information provided by the node degrees in the graph to encode expressive node representations. Theoretically, we demonstrate that SMILE can enhance the model generalization ability. Empirically, SMILE consistently outperforms other competitive models by a large margin across all evaluated datasets with in-domain and cross-domain settings. Our anonymous code can be found [here](#).

CCS Concepts

• Information systems → Data mining; • Computing methodologies → Neural networks.

*Key Laboratory of Symbolic Computation and Knowledge Engineering of the Ministry of Education

[†]Corresponding author

Permission to make digital or hard copies of all or part of this work for personal or classroom use is granted without fee provided that copies are not made or distributed for profit or commercial advantage and that copies bear this notice and the full citation on the first page. Copyrights for components of this work owned by others than the author(s) must be honored. Abstracting with credit is permitted. To copy otherwise, or republish, to post on servers or to redistribute to lists, requires prior specific permission and/or a fee. Request permissions from permissions@acm.org.

WWW '25, April 28-May 2, 2025, Sydney, NSW, Australia

© 2025 Copyright held by the owner/author(s). Publication rights licensed to ACM.
ACM ISBN 979-8-4007-1274-6/25/04

<https://doi.org/10.1145/3696410.3714905>

Keywords

Graph neural network, Few-shot learning, Node classification

ACM Reference Format:

Yonghao Liu, Mengyu Li, Fausto Giunchiglia, Lan Huang, Ximing Li, Xiaoyue Feng, and Renchu Guan. 2025. Dual-level Mixup for Graph Few-shot Learning with Fewer Tasks. In *Proceedings of the ACM Web Conference 2025 (WWW '25)*, April 28-May 2, 2025, Sydney, NSW, Australia. ACM, New York, NY, USA, 11 pages. <https://doi.org/10.1145/3696410.3714905>

1 Introduction

As a fundamental data structure, graphs can effectively model complex relationships between objects and they are ubiquitous in the real world. Graph neural networks (GNNs) have been widely employed as an effective tool for graph task analysis [10, 17, 19, 22–26, 29–32]. Prevailing GNN models are designed under the supervised learning paradigm, which implies that they require abundant labeled data to achieve satisfactory classification performance [4, 44]. Given the limited number of labeled nodes per class, known as few-shot cases [27, 57], these models suffer from severe overfitting, leading to a significant performance decline [14, 21].

Meta-learning has emerged as a viable option for effectively learning from limited labeled data. Its core concept is to train on tasks instead of instances as training units, aiming to capture the differences between tasks to enhance the model generalizability [13]. Several pioneering models [49, 59] have attempted to leverage integrate GNNs and meta-learning techniques to address graph few-shot learning problems. However, these graph meta-learning models all assume the existence of abundant accessible meta-training tasks to extract generalizable meta-knowledge for rapid adaptation to meta-testing tasks with only a few labeled instances. In other words, their outstanding performance critically depends on a wide range of meta-training tasks. For many real-world applications, due to the difficulty of task generation or data collection, we may not be able to obtain an adequate number of meta-training tasks [18, 44, 55]. For molecular property prediction, labeling newly discovered chemical compounds requires extensive domain knowledge and expensive wet-lab experiments [11]. Moreover, even after annotation, the currently known chemical properties (*i.e.*, classes)

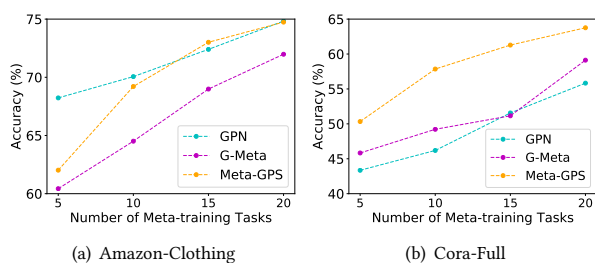


Figure 1: Model performance varies with the number of meta-training tasks across different datasets.

are limited, encompassing only common molecular characteristics such as polarity, solubility, and toxicity [33].

To further support our argument, we select three representative graph meta-learning models (*i.e.*, GPN [4], G-Meta [14], and Meta-GPS [27]) and evaluate their performance under varying numbers of meta-training tasks in Fig. 1. We distinctly observe that as the number of available meta-training tasks decreases, the overall performance of all methods greatly deteriorates. Because they tend to memorize meta-training tasks directly, which significantly constrains their generalization ability to novel tasks in the meta-testing stage [40]. This naturally raises a pressing question for us in more realistic scenarios: *How can we perform graph few-shot learning in scenarios with fewer tasks to extract as much transferable meta-knowledge as possible, thereby enhancing the model generalization performance?* Regarding this, although some recent studies [16, 43] have made some efforts on this issue, they primarily employ intricate network architectures to endow models with favorable characteristics, yet there is still room for improvement. We argue that there are two serious issues for our focused scenarios, which greatly hamper the model performance. *On the one hand*, there are only limited support samples available for training within each meta-training task, which complicates the accurate reflection of the real data distribution. Therefore, it poses a challenge for the model to effectively capture the data characteristics, severely affecting its inductive bias capability [37]. *On the other hand*, when there are only limited meta-training tasks available, the model tends to directly fit the biased task distribution. This implies not only a shortage of data for each task, but also a reduced number of available tasks. The combined effect of these two factors increases the unnecessary oscillation during predictions outside the training examples, leading to reduced generalization capability.

To address these issues mentioned above, we develop a **SiMple** yet **effectIve** approach for graph few-shot Learning with **fEwer** tasks, namely, **SMILE**. Specifically, given the graph data, we first obtain discriminative node embeddings using our designed graph encoder. In this process, we introduce node degrees as prior information to fully utilize valuable information present in the existing graph. Then, we introduce a dual-level mixup strategy that operates on the obtained hidden node representations, consisting of both within-task and across-task mixup. The former involves random sampling of two instances from the same category within a task and applies linear interpolation to generate new samples, thereby

enriching the data distribution. The latter requires computing class prototypes in two randomly selected original meta-training tasks, and then linearly interpolating class prototypes from different tasks to generate new tasks, thereby densifying the task distribution. These two employed strategies effectively mitigate the adverse effects caused by sample and task scarcity. Empirically, despite its simplicity and the absence of sophisticated techniques, the proposed approach demonstrates remarkable performance. Furthermore, we provide a theoretical elucidation of the underlying mechanism of our method, demonstrating its ability to constrict the upper bound of generalization error and consequently achieve superior generalization. In summary, our contributions can be summarized as follows:

- We propose a simple yet effective approach, SMILE, which leverages dual-level task mixup technique and incorporates the node degrees prior information, for graph few-shot learning with fewer tasks.
- We theoretically analyze the reasons why our approach works, demonstrating its ability to enhance generalization performance by regularizing model weights.
- We conduct extensive experiments on the several datasets, and the results show that SMILE can considerably outperform other competitive baselines by a large margin with in-domain and cross-domain settings.

2 Related Work

2.1 Few-shot Learning

Few-shot learning aims to quickly adapt meta-knowledge acquired from previous tasks to novel tasks with only a small number of labeled samples, thereby enabling few-shot generalization of machine learning algorithms [5, 6, 13]. Typically, there are three main strategies to solve few-shot learning. Some methods [35, 42, 47] utilize prior knowledge to constrain the hypothesis space at the *model level*, learning a reliable model within the resulting smaller hypothesis space. A series of methods [7–9, 38, 41] improve the search strategy at the *algorithm level* by providing good initialization or guiding the search steps. Another line of works [12, 53, 54] augment tasks at the *data level* to obtain precise empirical risk minimizers. For the few-shot learning with limited tasks, there are various explorations in Euclidean data, such as images and texts. For example, TAML [15] and MR-MAML [56] directly apply regularization on the few-shot learner to reduce their reliance on the number of tasks. Meta-aug [40] and MetaMix [54] perform data augmentation on individual tasks to enrich the data distribution. MLTI [55] and Meta-Inter [18] directly generate source tasks to densify the task distribution.

2.2 Graph Few-shot Learning

Inspired by the success of few-shot learning in computer vision [2, 20, 46] and natural language processing [1, 36, 48], few-shot learning on graphs has recently seen significant development [23, 25, 27, 28, 43, 49, 50]. The core concept of current mainstream methods is to develop complicated algorithms to address the problem of few-shot learning on graphs. For instance, Meta-GNN [59], G-Meta [14], and Meta-GPS [27] are all subjected to specific modifications

based on the MAML [5] algorithm, employing a bi-level optimization strategy to learn better parameter initialization. While the above models yield fruitful results, their reliance on substantial and diverse of meta-training tasks, coupled with their high complexity, has impeded their further advancement. Recently, TLP [44] and TEG [16] attempt to alleviate the limited diversity in meta-training datasets by using graph contrastive learning and equivariant neural networks, respectively. With the aid of sophisticated network designs, these methods have yielded promising results in graph few-shot scenarios. However, there is little effort to address the graph few-shot learning problem from the perspective of data augmentation.

3 Method

In this section, we first present the preliminary knowledge. Then, we detail our proposed SMILE, which consists of two components: node representation learning and dual-level mixup strategy. To facilitate better understanding, we present the overall framework of the model in Fig. 2.

3.1 Preliminary

Given a graph $\mathcal{G} = \{\mathcal{V}, \mathcal{E}, Z, A\}$, \mathcal{V} and \mathcal{E} represent the sets of nodes and edges, respectively. $Z \in \mathbb{R}^{n \times d}$ is the feature matrix of nodes and $A \in \mathbb{R}^{n \times n}$ is the corresponding adjacency matrix. Our model adheres to the prevalent meta-learning training paradigm, which involves training on sampled tasks. In this work, we mainly focus on few-shot node classification, which is the most prevailing and representative task in graph few-shot learning. Moreover, we highlight that in our focused scenarios, the number of available meta-training tasks sampled from an unknown task distribution is extremely small compared to traditional experimental settings, referred to as *few-shot node classification with fewer tasks*. Our goal is to enable the model to effectively extract meta-knowledge even from such limited tasks, which can generalize to novel tasks in the meta-testing phase. For better understanding, we summarize the main symbols of this work in **Appendix A**.

3.2 Node Representation Learning

Generally, the initial step involves encoding the nodes within the graph into a latent space, thereby transforming them into low-dimensional hidden vectors. GNNs have become the foremost choice for node embedding due to its powerful representational capabilities on graphs. It follows a message-passing mechanism, continuously aggregating messages from neighboring nodes to iteratively update the embedding of the target node. Guided by the simple philosophy, we adopt the SGC model [52] to learn node embeddings. Specifically, which can be defined as:

$$H = \check{A} \dots \check{A} Z W^{(0)} W^{(1)} \dots W^{(\ell-1)} = \check{A}^\ell Z W^*, \quad (1)$$

where $\check{A} = \hat{D}^{-1/2} \hat{A} \hat{D}^{-1/2}$ is the symmetric normalized adjacency matrix with added self-loops, *i.e.*, $\hat{A} = A + I$. $\hat{D}_i = \sum_j \hat{A}_{i,j}$ denotes the corresponding degree matrix. W^* is the collapsing weight matrices. After performing graph convolution operations, we can obtain the node vectors $H \in \mathbb{R}^{n \times d}$ that simultaneously encode node features and topology structure.

Given that few-shot models are highly noise-sensitivity [58], it is necessary to incorporate more prior knowledge to refine representations. Such prior knowledge is often reflected on node degree about the node popularity and importance [39]. Therefore, we consider explicitly incorporating it to evaluate each node. Specifically, we first adopt another SGC to derive the interaction weights $\kappa \in \mathbb{R}^{n \times 1}$ for all nodes. Then, based on the node degree information, we obtain the node centralities $\alpha \in \mathbb{R}^{n \times 1}$ to perform degree normalization for adjusting κ . Finally, we acquire the refined node representations $X \in \mathbb{R}^{n \times d}$ using the adjusted scores $\beta \in \mathbb{R}^{n \times 1}$. The above procedures can be formulated as follows:

$$\begin{aligned} \kappa &= \check{A}^\ell Z W, & \alpha &= \log(\{\hat{D}_i\}_{i=1}^n), \\ \beta &= \text{softmax}(\delta(\alpha \odot \kappa)), & X &= \beta \odot H, \end{aligned} \quad (2)$$

where $W \in \mathbb{R}^{d \times 1}$ is the trainable parameters and $\delta(\cdot)$ is the sigmoid function. \odot denotes the element-wise product.

After completing the node representation learning, we introduce the few-shot setting by defining some key notations. The meta-training tasks $\mathcal{D}_{org} = \{\mathcal{T}_t\}_{t=1}^{T_{org}}$ are sampled from a task distribution $p(\mathcal{T})$, where each task contains a support set $\mathcal{S}_t = \{(X_{t,i}^s, Y_{t,i}^s)\}_{i=1}^{n_s}$ and a query set $\mathcal{Q}_t = \{(X_{t,i}^q, Y_{t,i}^q)\}_{i=1}^{n_q}$, denoted as $\mathcal{T}_t = \{\mathcal{S}_t, \mathcal{Q}_t\}$. Here, $X_{t,i}^s$ and $Y_{t,i}^s \in \mathcal{Y}_{tra}$ denote the node embeddings and its label, where \mathcal{Y}_{tra} denotes the set of base classes. For the meta-testing task $\mathcal{T}_{tes} = \{\mathcal{S}_{tes}, \mathcal{Q}_{tes}\} = \{\{(X_{tes,i}^s, Y_{tes,i}^s)\}_{i=1}^{n_s}, \{(X_{tes,i}^q, Y_{tes,i}^q)\}_{i=1}^{n_q}\}$, it is composed in the same way as the meta-training task \mathcal{T}_t , with the only difference being that the node label belong to the novel class set \mathcal{Y}_{tes} , which is disjoint from \mathcal{Y}_{tra} , *i.e.*, $\mathcal{Y}_{tra} \cap \mathcal{Y}_{tes} = \emptyset$. When the support set \mathcal{S}_{tes} consists of N sampled classes, each with K nodes, we refer to it as an N -way K -shot problem. The construction of \mathcal{Q}_{tes} is the same as \mathcal{S}_{tes} , except that each class has M nodes. Typically, the model is first trained on the meta-training tasks \mathcal{D}_{org} . During the meta-testing stage, the model is fine-tuned on \mathcal{S}_{tes} and then is evaluated the performance on \mathcal{Q}_{tes} .

3.3 Dual-level Mixup Strategy

If we directly conduct few-shot learning on the refined representations, the model's performance would be degraded due to overfitting and constrained generalization. Therefore, we introduce a dual-level mixup strategy, including within-task and across-task mixup, to deal with this issue. Next, we will provide detailed descriptions of each technique.

3.3.1 Within-task Mixup. Due to the exceedingly restricted number of sampled nodes in both the support set and query set for each task during the meta-training phase, the efficiency of the meta-training is considerably compromised. Hence, we propose using the within-task mixup strategy to generate more samples for increasing the diversity of the data. Concretely, for a given meta-training task \mathcal{T}_t , we perform random sampling on the support set \mathcal{S}_t and query set \mathcal{Q}_t , selecting two samples i and j from the same category k for linear interpolation to generate a new one r . The above procedure can be formulated as:

$$X_{t,r;k}^{r,s} = \lambda X_{t,i;k}^s + (1-\lambda) X_{t,j;k}^s, \quad X_{t,r;k}^{r,q} = \lambda X_{t,i;k}^q + (1-\lambda) X_{t,j;k}^q, \quad (3)$$

where $\lambda \in [0, 1]$ is sampled from the Beta distribution $Beta(\eta, \gamma)$ specified by η and γ .

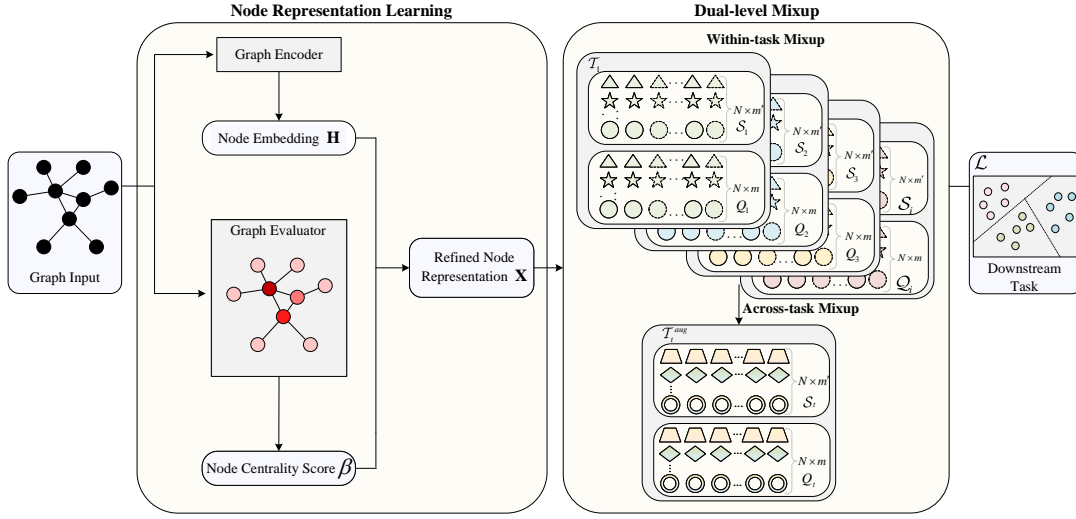


Figure 2: The overall architecture of SMILE.

Here, we do not perform label interpolation as the labels of the two sampled nodes are the same, resulting in identical labels for the generated node. There are two reasons for this. First, interpolating samples from different categories would make it difficult to compute prototypes of the mixed labels while expanding the node label space of the original task. Second, this would pose intricate troubles for the subsequent across-task interpolation.

We iteratively apply Eq.3 to generate the additional support set $S'_t = \{(X'_{t,i}, Y'_{t,i})\}_{i=1}^{n_{s'}}$ and query set $Q'_t = \{(X'_{t,i}, Y'_{t,i})\}_{i=1}^{n_{q'}}$, which are subsequently merged with the original corresponding sets to obtain the augmented task \mathcal{T}_t (To avoid introducing extra symbols, we consistently use \mathcal{T}_t to denote the task that undergoes within-task mixup in the following sections.), i.e., $\mathcal{T}_t = \{S_t \cup S'_t, Q_t \cup Q'_t\}$. The number of nodes in the amplified support and query sets of the augmented task \mathcal{T}_t are $m' = n_s + n_{s'}$ and $m = n_q + n_{q'}$, respectively.

3.3.2 Across-task Mixup. Solely conducting within-task mixup does not address the issue of the limited number of tasks. Therefore, we utilize across-task mixup to directly create new tasks, densifying the task distribution. Specifically, *in the first step*, we randomly select two tasks, \mathcal{T}_i and \mathcal{T}_j , from the given meta-training tasks $\mathcal{D}_{org} = \{\mathcal{T}_t\}_{t=1}^{T_{org}}$. *In the second step*, we randomly sample a class k from the support set S_i of \mathcal{T}_i and a class k' from the support set S_j of \mathcal{T}_j , and then compute class-specified support prototypes. This procedure can be expressed as:

$$C_{i;k}^s = \frac{1}{|S_{i;k}|} \sum_{(X_{i,\ell}^s, Y_{i,\ell}^s) \in S_i} \mathbb{I}_{Y_{i,\ell}^s = k} X_{i,\ell}^s, \quad (4)$$

$$C_{j;k'}^s = \frac{1}{|S_{j;k'}|} \sum_{(X_{j,\ell}^s, Y_{j,\ell}^s) \in S_j} \mathbb{I}_{Y_{j,\ell}^s = k'} X_{j,\ell}^s,$$

where $\mathbb{I}(\cdot)$ is the indicator function that is 1 when $Y_{i,\ell}^s = k$, and 0 otherwise. Similarly, we can obtain query prototypes $C_{i;k}^q$ for class k and $C_{j;k'}^q$ for class k' by applying Eq.4 to the query sets Q_i of \mathcal{T}_i and Q_j of \mathcal{T}_j .

In the third step, we individually perform feature-level linear interpolation on the support prototypes and query prototypes to generate new samples. Considering that different tasks have different label spaces, we directly treat the label associated with the interpolated data as a new class \tilde{k} . We can formulate the above process as:

$$\begin{aligned} \tilde{X}_{t,\ell;\tilde{k}}^s &= \lambda C_{i;k}^s + (1-\lambda) C_{j;k'}^s, & \tilde{Y}_{t,\ell;\tilde{k}}^s &= \Phi(Y_{i;k}^s, Y_{j;k'}^s), \\ \tilde{X}_{t,\ell;\tilde{k}}^q &= \lambda C_{i;k}^q + (1-\lambda) C_{j;k'}^q, & \tilde{Y}_{t,\ell;\tilde{k}}^q &= \Phi(Y_{i;k}^q, Y_{j;k'}^q), \end{aligned} \quad (5)$$

where $\Phi(\cdot, \cdot)$ represents the label uniquely determined by the pair (\cdot, \cdot) . We perform m' iterations for the support data and m iterations for the query data in Eq.5, i.e., $\{\tilde{X}_{t,\ell;\tilde{k}}^s, \tilde{Y}_{t,\ell;\tilde{k}}^s\}_{\ell=1}^{m'}$ and $\{\tilde{X}_{t,\ell;\tilde{k}}^q, \tilde{Y}_{t,\ell;\tilde{k}}^q\}_{\ell=1}^m$. Note that the sampled λ each time is different.

Finally, we repeat the second and third steps N times to construct an N -way m' -shot interpolation task $\mathcal{T}_t^{aug} = \{\tilde{S}_t, \tilde{Q}_t\} = \{\{\tilde{X}_{t,\ell;\tilde{k}}^s, \tilde{Y}_{t,\ell;\tilde{k}}^s\}_{\tilde{k}=1}^N, \{\tilde{X}_{t,\ell;\tilde{k}}^q, \tilde{Y}_{t,\ell;\tilde{k}}^q\}_{\tilde{k}=1}^N\}$. We can conduct the above process multiple times to obtain the interpolated tasks $\mathcal{D}_{aug} = \{\mathcal{T}_t^{aug}\}_{t=1}^{T_{aug}}$ and merge them with the original tasks \mathcal{D}_{org} to form the final meta-training tasks $\mathcal{D}_{all} = \mathcal{D}_{org} \cup \mathcal{D}_{aug}$. The number of tasks in \mathcal{D}_{all} is $T = T_{org} + T_{aug}$.

Model Training. After performing the dual-level mixup operation, we adopt a classic metric-based episodic training for few-shot node classification. We first derive the prototype C_k in the support set S_t of each task \mathcal{T}_t from \mathcal{D}_{all} with the manner shown in Eq.4.

Next, we optimize the parameters of the model by performing distance-based cross-entropy loss function on all query sets in \mathcal{D}_{all} as:

$$\mathcal{L} = \sum_{t=1}^T \sum_{i=1}^m \mathbb{I}_{Y_{t,i}=k} \log \frac{\exp(-d(\theta^\top X_{t,i}^q, C_k))}{\sum_{k'} \exp(-d(\theta^\top X_{t,i}^q, C_{k'}))}, \quad (6)$$

where $d(\cdot, \cdot)$ is the Euclidean distance function and θ is the trainable vector.

In the meta-testing stage, we do not perform any mixup operations for the evaluated task \mathcal{T}_{tes} . Actually, we first use the well-trained model to compute class prototypes on the support set, and then assign samples in the query set to their nearest prototype, defined as:

$$C_k = \frac{1}{|\mathcal{S}_{tes,k}|} \sum_{(X_{tes,i}^s, Y_{tes,i}^s) \in \mathcal{S}_{tes}} \mathbb{I}_{Y_{tes,i}=k} X_{tes,i}^s \quad (7)$$

$$Y_{tes,*}^q = \operatorname{argmin}_k d(\theta^\top X, C_k).$$

We present the process of proposed SMILE in **Appendix B**. The time complexity analysis of SMILE are presented in **Appendix C**.

4 Theoretical Analysis

In this section, we theoretically analyze why our proposed SMILE, equipped with intra-task and inter-task mixup, can alleviate overfitting and exhibit better generalization capabilities. We first present the obtained key points: *SMILE can regularize the weight parameters in a distribution-dependent manner and reduce the upper bound of the generalization gap by controlling the Rademacher complexity*. Next, we elaborate on the proposed theorems to support the aforementioned points. For simplicity, we conduct a detailed theoretical analysis of SMILE in the binary classification scenario, assuming the use of preprocessed centralized dataset that satisfies the condition $\mathbb{E}_X[X] = 0$. Moreover, the proposed SMILE can be modeled as $f_\theta(Z) = \theta^\top g_\zeta(Z) = \theta^\top X$, where $g_\zeta(\cdot)$ denotes the graph encoder parameterized by ζ . We consider using the loss from Eq.6 for tasks in \mathcal{D}_{all} . Particularly, the empirical loss function based on enriched training samples for binary classification can be simplified as:

$$\mathcal{L}(\mathcal{D}_{all}; \theta) = \sum_{t=1}^T \sum_{i=1}^m (1 + \exp(\langle X_{t,i}^q, -(C_1 + C_2)/2, \theta \rangle))^{-1}, \quad (8)$$

$$C_k = \frac{1}{|\mathcal{S}_{t,k}|} \sum_{(X_{t,i}^s, Y_{t,i}^s) \in \mathcal{S}_t} \mathbb{I}_{Y_{t,i}=k} X_{t,i}^s,$$

where $\langle \cdot, \cdot \rangle$ denote the dot product operation. The approximation of the loss function $\mathcal{L}(\mathcal{D}_{all}; \theta)$ in Eq.8 is formalized as:

$$\mathcal{L}(\mathcal{D}_{all}; \theta) \approx \mathcal{L}(\mathcal{D}_{org}; \theta) + \mathcal{L}(\bar{\lambda} \mathcal{D}_{org}; \theta) + \mathcal{M}(\theta), \quad (9)$$

where $\bar{\lambda} = \mathbb{E}_{\rho_\lambda}[\lambda]$ and $\mathcal{M}(\theta)$ is a quadratic regularization term with respect to θ , defined as:

$$\mathcal{M}(\theta) = \mathbb{E}_{\mathcal{T}_i \sim p(\mathcal{T})} \mathbb{E}_{(X_t, Y_t) \sim q(\mathcal{T}_i)} \frac{\phi(P_t)(\phi(P_t) - 0.5)}{2(1 + \exp(P_t))} (\theta^\top \Sigma_X \theta) \quad (10)$$

in which $P_t = \langle X_t^q - (C_1 + C_2)/2, \theta \rangle$, $\phi(P_t) = \exp(P_t)/(1 + \exp(P_t))$, and $\Sigma_X = \mathbb{E}[XX^\top] = \frac{1}{m} \sum_{i=1}^m X_i X_i^\top$.

Eq.9 shows that SMILE imposes an additional regularization term on the trainable weights to constrain the solution space, thereby reducing the likelihood of overfitting.

To define the generalization gap problem formally, we introduce a function class of the dual form related to the regularization term in Eq.9, as shown in Eq.11.

$$\mathcal{F}_v = \{X \rightarrow \theta^\top X : \theta^\top \Sigma_X \theta \leq v\}. \quad (11)$$

Moreover, we represent the expected risk R and empirical risk \hat{R} as follows:

$$R = \mathbb{E}_{\mathcal{T}_i \sim p(\mathcal{T})} \mathbb{E}_{(X_j, Y_j) \sim q(\mathcal{T}_i)} \mathcal{L}(f_\theta(X_j), Y_j), \quad (12)$$

$$\hat{R} = \mathbb{E}_{\mathcal{T}_i \sim \hat{p}(\mathcal{T})} \mathbb{E}_{(X_j, Y_j) \sim \hat{q}(\mathcal{T}_i)} \mathcal{L}(f_\theta(X_j), Y_j).$$

Then, we present the following theorem for improved generalization gap brought by SMILE.

Theorem 4.1. *Assume that X, Y and θ are bounded. For all $f \in \mathcal{F}_v$, where θ satisfies $\theta^\top \Sigma_X \theta \leq v$, we have the following generalization gap bound, with probability at least $(1 - \epsilon)$ over the training samples,*

$$|\hat{R} - R| \leq 2 \left(\sqrt{\frac{v \cdot \operatorname{rank}(\Sigma_X)}{m}} + \sqrt{\frac{v}{T}} \left(\operatorname{rank}(\Sigma_X) \right) \right) \quad (13)$$

$$+ 3 \left(\sqrt{\frac{\log(2/\epsilon)}{2m}} + \sqrt{\frac{\log(2/\epsilon)}{2T}} \right),$$

where m and T denote the number of nodes in the query set and the number of meta-training tasks.

Based on Theorem 4.1, we can obtain several in-depth findings. On the one hand, SMILE induces a regularized weight space for θ , leading to a smaller v . On the other hand, the introduced intra-task and inter-task interpolations increase m and T simultaneously. These two aspects work together to reduce the upper bound of the generalization gap of SMILE and alleviate overfitting.

According to the above theorem, we can naturally confirm the following corollary.

Corollary 4.2. *Let $|\hat{R} - R|$ and $|\hat{R}_{ori} - R_{ori}|$ denote the model generalization bounds trained under our proposed task augmentation strategy and standard training strategy, respectively. We have the following inequality holding,*

$$U(|\hat{R} - R|) \leq U(|\hat{R}_{ori} - R_{ori}|), \quad (14)$$

where $U(\cdot)$ denotes the operation of taking the upper bound.

Corollary 4.2 suggests that SMILE achieves tight generalization bound than other models trained in a standard way.

Suppose the empirical distribution of source tasks in the meta-training be $\hat{\mathbb{P}}$ and the expected distribution of the query set of target tasks be \mathbb{Q} , then during the adaptation process, we expect to reduce the data-dependent upper bound, defined as $\sup_{f \in \mathcal{F}} |\mathbb{E}_{\hat{\mathbb{P}}} - \mathbb{E}_{\mathbb{Q}}|$.

Empirically, when source tasks and target tasks are more similar, the model is more likely to extract generalizable meta-knowledge from source tasks to quickly adapt to target tasks. Theoretically, we present the Theorem 4.3, which demonstrates the reduction of the upper bound between $\hat{\mathbb{P}}$ and \mathbb{Q} induced by our proposed strategy.

Theorem 4.3. *Assume the source tasks and target tasks are drawn from distribution $\hat{\mathbb{P}}$ and \mathbb{Q} , and they are independent. For $\epsilon > 0$, with probability at least $(1 - \epsilon)$ over the draws of samples, we have the following upper bound between data distributions,*

$$\sup_{f \in \mathcal{F}} |\mathbb{E}_{\hat{\mathbb{P}}} - \mathbb{E}_{\mathbb{Q}}| \leq \left(2\sqrt{v \cdot \operatorname{rank}(\Sigma_X)} + \sqrt{\frac{\log(1/\epsilon)}{2}} \right) \left(\sqrt{\frac{1}{m}} + \sqrt{\frac{1}{n_q}} \right), \quad (15)$$

where n_q denotes the number of nodes in the query set of the meta-testing task.

We can draw the conclusion that the introduction of intra-task interpolation leads to an increase in the value of m . Additionally, according to Eq.9, the regularization effect can result in a decrease of v . Consequently, Theorem 4.3 suggests that our method has the capability to diminish the disparity between the distributions of the source task and target task, facilitating the extraction of pertinent knowledge and, in turn, enhancing the model’s generalization.

5 Experiment

Datasets. To demonstrate the effectiveness of our approach, we conduct few-shot node classification with fewer tasks on four selected prevalent datasets widely used by previous researches, including **Amazon-Clothing** [34], **CoraFull** [3], **Amazon-Electronics** [34], and **DBLP** [45]. Table 1 shows the statistics of these datasets. Concisely, # Nodes and # Edges represent the number of nodes and edges in the dataset, respectively. # Features denotes the dimension of the initialized node features, and # Labels is the number of classes. Class Splits represents the number of classes used for meta-training/meta-validation/meta-testing. The detailed descriptions of these evaluated datasets can be found in **Appendix D**.

Table 1: Statistics of the datasets.

Dataset	# Nodes	# Edges	# Features	# Labels	Class Splits
Amazon-Clothing	24,919	91,680	9,034	77	40/17/20
Cora-Full	19,793	65,311	8,710	70	25/20/25
Amazon-Electronics	42,318	43,556	8,669	167	90/37/40
DBLP	40,672	288,270	7,202	137	80/27/30

Baselines. We mainly select three types of baselines for comparison to verify the superiority of the proposed SMILE. *Traditional meta-learning* methods consist of **Protonet** [42] and **MAML** [5]. *Meta-learning with fewer tasks* methods comprise **MetaMix** [54], **MLTI** [55], and **Meta-Inter** [18]. *Graph meta-learning* methods include **Meta-GNN** [59], **GPN** [4], **G-Meta** [14], **Meta-GPS** [27], **X-FNC** [50], **COSMIC** [51], **TLP** [44], and **TEG** [16]. The descriptions and implementations of these baselines are provided in **Appendix E**.

Implementation Details. In the *node representation learning* stage, we adopt 2-layer SGC with 16 hidden units. In the *dual-level mixup* stage, we uniformly set the two parameters involved in the beta distribution to 0.5, i.e., $\eta = \gamma = 0.5$. Moreover, in within-task mixup, we generate the same number of nodes as the original support and query set in each meta-training task by default, that is, $n_{s'} = n_s$, $n_{q'} = n_q$. In across-task mixup, we generate as many interpolated tasks as original tasks, that is $T_{aug} = T_{org}$. In the cross-domain setting, we meta-train the model on one source domain and then meta-test it on another target domain. To ensure fair comparison, we perform meta-training on the same sampled tasks for all models. Moreover, we evaluate the performance of our model using the average accuracy (Acc) and macro-F1 (F1) score across 50 randomly selected meta-testing tasks.

6 Result

Model Performance. We present the results of our proposed SMILE and other models under both *in-domain* and *cross-domain* settings with different number of tasks across several datasets in

Tables 2 and 3. According to above results, we can obtain the following in-depth analysis. We can find that our approach achieves the best performance across varying numbers of meta-training tasks in both in-domain and cross-domain settings for all datasets, demonstrating its superiority in dealing with graph few-shot learning with fewer tasks. One plausible reason is that we explicitly introduce degree-based prior in the node representation stage, resulting in more discriminative features beneficial for subsequent tasks. Furthermore, we employ a dual-level mixup strategy, enriching the diversity of both within-task and across-task data, effectively alleviating the negative impact of data and task scarcity. These strategies facilitate the model to extract more transferable meta-knowledge, thereby greatly enhancing its generalization capability.

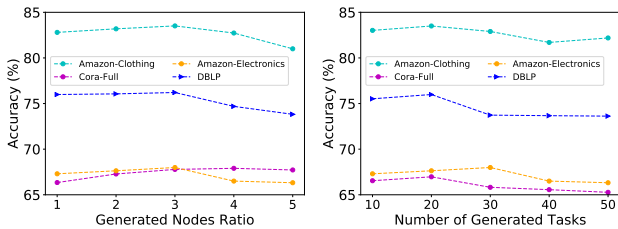
We find that graph meta-learning models represented by COSMIC and TEG perform well in scenarios with more tasks across multiple datasets, which aligns with our expectations. These models are specifically designed for graph few-shot learning and utilize unique few-shot algorithms that enable them to achieve discriminative node representations with limited labeled data. However, they struggle in scenarios with fewer tasks, performing significantly worse than our model. This is because they can only extract sufficient transferable meta-knowledge when there are ample meta-training tasks. Moreover, the meta-learning with fewer tasks models equipped with SGC, such as MLTI and Meta-Inter, also demonstrate impressive performance in the both in-domain and cross-domain experimental settings. We attribute this phenomenon to the specific strategies employed by these models to mitigate the negative effects caused by limited tasks. However, this type of models still significantly lag behind our model, as they do not incorporate degree-based prior knowledge and fail to address scarcity issues from both data and task perspectives simultaneously. Additionally, traditional meta-learning methods consistently underperform compared to other methods because they completely overlook the important structural information in the graph.

Ablation Study. To demonstrate the effectiveness of our adopted strategies, we design several model variants. (I) *vanilla mixup*: Without the dual-level mixup, we first compute the prototypes using the support set, and then perform vanilla mixup to query set, which involves mixing the features and generates soft labels. (II) *internal mixup*: In the absence of dual-level mixup, we directly perform mixup on different classes within each task and generate corresponding hard labels, treating them as novel classes. (III) *w/o within and across*: We simultaneously discard both within-task and across-task mixup operations. (IV) *w/o within*: We delete the within-task operation and leave the across-task one. (V) *w/o across*: We remove the across-task strategy and retain the within-task one. (VI) *w/o degree*: We exclude the utilization of degree information and solely employ the vanilla SGC for node representation learning.

According to Table 4, it is evident that the employed strategies have a favorable impact on the model performance. The introduction of dual-level mixup enriches the samples within each task and provides diverse tasks, making significant contributions to enhancing the model. The adopted degree-based prior information also improves the model by learning expressive node embeddings, especially in cross-domain setting. When removing the degree information, the performance drastically declines. One plausible reason is that this module explicitly utilizes structural prior knowledge from

Table 2: Results (%) of different models using fewer tasks on datasets under the 5-way 5-shot *in-domain* setting. Bold: best (based on the pairwise t-test with 95% confidence). Underline: runner-up.

Model	Amazon-Clothing								CoraFull							
	5 tasks		10 tasks		15 tasks		20 tasks		5 tasks		10 tasks		15 tasks		20 tasks	
	Acc	F1	Acc	F1	Acc	F1	Acc	F1	Acc	F1	Acc	F1	Acc	F1	Acc	F1
Protonet	49.17	48.36	53.51	52.55	55.82	54.99	57.99	57.14	37.20	35.98	40.14	38.89	43.90	42.96	45.58	44.34
MAML	44.90	43.66	45.67	44.44	46.29	44.97	46.90	45.60	38.15	36.83	42.26	41.28	44.21	43.95	46.37	45.43
MetaMix	78.32	78.22	78.66	78.52	80.16	79.15	81.09	80.52	62.95	62.25	64.20	63.95	65.72	64.19	67.59	66.26
MLTI	79.19	78.59	79.91	78.92	80.22	79.39	81.27	80.86	63.19	63.06	65.72	65.69	66.25	64.92	67.15	66.10
Meta-Inter	<u>79.92</u>	<u>79.22</u>	<u>80.12</u>	<u>79.56</u>	<u>80.55</u>	<u>79.90</u>	<u>81.26</u>	<u>81.05</u>	<u>63.82</u>	<u>63.36</u>	66.59	65.92	67.19	65.50	68.22	67.59
Meta-GNN	55.29	50.44	57.19	53.65	62.29	59.55	70.19	67.22	42.96	40.83	45.09	42.87	47.15	45.38	49.88	48.12
GPN	68.23	67.16	70.06	69.57	72.40	71.95	72.81	71.56	43.35	42.08	46.19	44.81	51.56	50.24	55.83	54.76
G-Meta	60.43	60.11	64.51	63.74	68.99	67.96	71.98	72.75	45.84	44.27	49.22	48.91	51.15	50.53	59.12	58.56
Meta-GPS	62.02	59.76	69.21	69.04	73.01	71.92	75.74	74.85	50.33	48.22	57.85	54.86	61.28	60.11	63.76	62.28
X-FNC	69.12	68.29	72.12	71.11	75.19	74.63	79.26	78.02	55.06	53.10	61.53	60.29	65.22	64.10	66.09	65.12
COSMIC	75.66	74.92	76.39	75.72	77.92	76.59	78.36	77.39	62.29	60.39	65.39	64.80	66.72	65.72	68.29	67.20
TLP	71.39	70.39	73.39	72.52	74.72	73.36	75.60	74.29	51.79	49.72	56.72	55.79	57.72	56.73	57.99	57.30
TEG	78.55	77.92	80.26	79.30	80.82	79.99	81.19	80.16	62.89	61.26	<u>68.29</u>	<u>67.39</u>	<u>68.59</u>	<u>67.55</u>	<u>70.06</u>	<u>69.29</u>
SMILE	82.80	82.49	83.46	82.88	83.92	83.33	84.66	84.52	66.34	65.70	71.72	71.15	70.78	70.19	72.60	72.10
Model	Amazon-Electronics								DBLP							
	5 tasks		10 tasks		15 tasks		20 tasks		5 tasks		10 tasks		15 tasks		20 tasks	
	Acc	F1	Acc	F1	Acc	F1	Acc	F1	Acc	F1	Acc	F1	Acc	F1	Acc	F1
Protonet	46.20	45.09	49.56	48.57	51.98	51.05	54.03	53.20	46.57	45.47	50.90	49.81	51.02	49.74	52.09	51.05
MAML	34.34	33.42	34.76	33.76	35.42	34.41	35.91	34.95	39.71	38.86	40.34	39.58	40.70	39.85	41.31	40.58
MetaMix	61.96	61.82	63.72	63.66	65.19	64.92	66.15	65.72	72.12	71.15	73.19	72.12	75.16	73.95	76.22	74.79
MLTI	62.25	62.02	65.26	65.09	66.72	65.59	67.19	66.22	72.36	71.96	72.92	72.55	73.22	73.10	75.10	74.95
Meta-Inter	62.79	62.56	65.76	65.52	67.19	66.15	68.99	67.29	72.52	72.11	73.19	72.99	74.28	73.25	75.29	75.10
Meta-GNN	40.52	39.74	46.16	45.87	48.92	47.93	50.86	50.07	50.68	49.04	53.86	49.67	59.72	59.36	65.49	62.12
GPN	49.08	47.91	51.12	49.98	54.24	53.23	56.69	55.62	70.26	69.13	<u>74.42</u>	<u>73.48</u>	<u>76.02</u>	<u>75.03</u>	<u>76.61</u>	<u>75.60</u>
G-Meta	43.29	42.20	49.57	52.90	56.96	55.38	60.41	59.91	53.08	48.13	55.92	53.64	57.82	56.76	63.17	62.85
Meta-GPS	46.11	43.62	57.90	56.20	67.73	66.69	70.13	69.15	56.59	54.12	65.20	63.20	73.00	72.35	75.16	73.19
X-FNC	59.26	56.39	63.72	62.10	<u>69.82</u>	67.63	71.36	70.02	69.06	68.10	72.53	71.29	74.29	73.22	76.19	75.20
COSMIC	64.06	63.02	<u>67.36</u>	<u>66.32</u>	68.22	67.09	70.16	69.30	71.29	70.19	72.09	70.80	73.02	71.20	75.16	72.22
TLP	63.09	62.19	64.30	63.59	65.72	64.32	67.18	66.72	71.26	70.75	72.87	72.09	73.39	73.06	75.16	74.69
TEG	<u>65.90</u>	<u>64.62</u>	67.29	66.22	69.80	<u>68.29</u>	<u>72.12</u>	<u>71.16</u>	<u>72.59</u>	<u>72.26</u>	73.79	72.19	75.52	74.50	76.26	75.12
SMILE	67.30	66.30	70.76	70.05	73.48	72.66	75.42	75.42	75.88	75.05	76.64	75.77	79.56	78.77	80.50	79.61

**Figure 3: Results vary with hyperparameters.**

the target graph domain, benefiting downstream tasks. Additionally, the results of model variants I and II demonstrate that performing label interpolation within each task, whether generating soft or hard labels, degrades the model performance.

Hyperparameter Sensitivity. In the 5-way 5-shot *in-domain* setting, we investigate the impact of two primary hyperparameters on the model performance: the ratio of generated nodes to the

original nodes per task (i.e., $\frac{n'_s+n'_q}{n_s+n_q}$), and the number of generated tasks T_{aug} . Notably, when the studied hyperparameter changes, we set others to their default values. The results are presented in Fig. 3. We can observe that both parameters demonstrate similar trends, with the model performance showing an initial increase followed by a decrease. We attribute this behavior to the substantial enrichment of data diversity by increasing the number of nodes within each task or the number of tasks. However, beyond a certain threshold, the introduced additional data fails to further densify the data distribution, resulting in limited information gain.

7 Conclusion

In this work, we propose a simple yet effective approach, called SMILE, for graph few-shot learning with fewer tasks. Specifically, we introduce a novel dual-level mixup strategy, including within-task and across-task mixup, for enriching the diversity of nodes within each task and the diversity of tasks. Also, we incorporate

Table 3: Results (%) of different models using fewer tasks on datasets under the 5-way 5-shot cross-domain setting. A→B denotes the model is trained on A and evaluated on B.

Dataset	Amazon-Clothing→CoraFull								CoraFull→Amazon-Clothing							
	5 tasks		10 tasks		15 tasks		20 tasks		5 tasks		10 tasks		15 tasks		20 tasks	
	Acc	F1	Acc	F1	Acc	F1	Acc	F1	Acc	F1	Acc	F1	Acc	F1	Acc	F1
Protonet	20.72	7.90	22.84	10.89	29.70	15.91	32.96	18.19	24.84	13.18	29.96	22.49	32.84	26.01	34.58	29.90
MAML	20.40	13.51	20.74	13.19	26.68	12.22	30.19	15.92	23.56	12.10	27.35	20.16	30.19	23.95	32.96	27.96
MetaMix	31.96	28.76	33.12	31.22	35.22	33.19	37.15	35.55	34.76	31.66	36.25	33.69	39.72	37.16	41.26	39.25
MLTI	33.29	30.12	35.16	32.29	38.25	35.52	40.22	38.29	35.12	33.49	37.22	35.29	42.19	41.52	45.66	43.95
Meta-Inter	34.72	32.19	35.76	34.26	40.16	37.59	42.29	40.32	41.76	39.59	43.22	41.57	44.11	42.25	47.29	45.55
Meta-GNN	26.36	20.99	30.50	26.72	33.22	30.15	35.99	32.16	32.16	22.39	35.22	26.62	38.16	29.35	39.66	32.90
GPN	35.86	34.81	39.38	38.03	41.10	39.82	41.96	41.15	40.08	38.73	41.78	40.67	43.90	42.87	45.04	44.30
G-Meta	30.36	26.95	33.19	29.62	35.29	33.16	36.21	35.20	35.22	30.16	37.22	30.29	40.19	32.29	41.19	36.96
Meta-GPS	32.02	27.07	34.15	30.19	35.66	34.15	39.26	37.55	45.59	43.29	47.62	45.10	50.19	47.12	52.19	49.32
X-FNC	33.59	31.10	35.15	32.19	37.25	34.12	39.72	36.29	47.26	45.16	49.30	46.22	52.20	49.29	53.72	50.22
COSMIC	<u>38.02</u>	36.22	40.09	37.05	<u>42.20</u>	39.09	<u>42.46</u>	40.30	49.20	47.19	52.02	51.29	53.09	52.16	<u>55.39</u>	<u>53.90</u>
TLP	37.99	<u>37.29</u>	<u>41.23</u>	<u>39.59</u>	41.99	<u>40.92</u>	<u>42.26</u>	<u>41.25</u>	<u>51.12</u>	<u>50.15</u>	<u>53.90</u>	<u>52.29</u>	<u>54.26</u>	<u>52.66</u>	<u>55.20</u>	<u>53.30</u>
TEG	33.05	31.29	<u>35.26</u>	<u>34.32</u>	35.80	<u>34.69</u>	36.35	35.36	41.09	40.20	42.12	41.39	43.72	42.60	46.56	43.87
SMILE	42.64	41.27	45.14	43.69	45.88	44.10	46.72	45.65	56.36	55.25	58.84	57.53	59.08	57.96	59.38	58.25
Dataset	Amazon-Electronics→DBLP								DBLP→Amazon-Electronics							
	5 tasks		10 tasks		15 tasks		20 tasks		5 tasks		10 tasks		15 tasks		20 tasks	
	Acc	F1	Acc	F1	Acc	F1	Acc	F1	Acc	F1	Acc	F1	Acc	F1	Acc	F1
Protonet	31.86	22.56	32.58	23.73	35.90	32.76	39.88	35.71	28.84	18.62	30.54	20.08	33.10	22.37	35.46	25.20
MAML	29.17	19.13	30.10	22.15	32.97	25.98	35.25	29.11	26.59	17.99	28.36	19.29	30.02	20.15	32.16	22.16
MetaMix	40.16	35.68	43.25	41.69	45.19	43.12	49.12	43.59	37.70	35.22	40.20	39.09	42.25	40.16	44.19	42.20
MLTI	42.12	37.19	46.39	45.06	49.19	47.25	51.35	50.39	38.22	36.96	41.39	40.25	43.39	42.05	46.12	45.09
Meta-Inter	46.19	45.12	48.15	46.79	51.29	49.76	53.18	51.02	41.50	40.15	43.19	41.10	45.20	43.35	47.15	45.05
Meta-GNN	39.19	34.72	42.26	39.16	43.96	39.55	45.66	42.19	35.72	33.20	39.59	38.62	40.39	39.29	41.26	40.22
GPN	<u>60.08</u>	<u>58.75</u>	<u>61.92</u>	<u>61.58</u>	<u>63.19</u>	<u>62.60</u>	<u>63.99</u>	<u>63.10</u>	42.99	41.46	<u>46.36</u>	<u>44.73</u>	<u>47.09</u>	<u>45.42</u>	<u>47.52</u>	<u>45.76</u>
G-Meta	45.72	43.32	47.22	45.09	47.96	45.99	49.56	48.39	37.22	35.93	40.19	39.52	42.35	40.19	43.62	42.19
Meta-GPS	47.59	46.70	49.20	47.16	50.26	49.96	52.39	51.22	<u>43.06</u>	<u>42.05</u>	45.12	43.16	46.02	44.95	46.79	45.02
X-FNC	49.19	48.36	49.55	48.02	51.35	50.26	52.90	51.39	41.59	40.02	42.36	42.19	44.16	43.16	46.39	45.25
COSMIC	57.22	55.30	58.29	57.35	60.20	61.19	61.36	62.30	39.20	37.11	41.02	40.22	43.03	42.22	44.32	43.26
TLP	58.25	57.19	59.33	59.01	61.29	60.02	62.16	61.25	41.11	40.16	43.20	42.25	44.16	42.32	45.20	43.90
TEG	38.05	36.29	40.21	39.32	42.80	41.69	43.35	42.36	33.19	31.20	34.22	33.52	35.70	34.62	36.55	35.37
SMILE	62.44	61.66	64.54	64.16	65.04	64.43	65.78	65.42	46.24	44.54	48.82	47.26	49.26	47.70	49.52	47.88

Table 4: Results of different model variants with respect to 5 tasks under the 5-way 5-shot setting.

Dataset	Clothing		Electronics		DBLP		CoraFull		Clothing→CoraFull		CoraFull→Clothing		Electronics→DBLP		DBLP→Electronics	
	Acc	F1	Acc	F1	Acc	F1	Acc	F1	Acc	F1	Acc	F1	Acc	F1	Acc	F1
vanilla mixup	78.82	78.45	60.98	60.70	74.06	73.03	61.90	61.07	38.90	38.26	52.93	52.29	57.92	57.30	40.52	39.26
internal mixup	78.96	78.72	63.59	62.21	75.34	74.45	63.64	63.00	39.12	38.59	53.22	53.19	59.02	57.96	41.36	40.56
w/o within and across	79.10	78.97	62.36	61.08	73.14	72.36	62.44	61.85	39.72	39.19	53.58	52.42	59.34	58.94	42.12	41.41
w/o within	80.72	80.93	65.96	64.99	75.44	74.59	64.06	63.40	40.28	39.63	54.52	53.50	60.86	59.16	42.28	41.79
w/o across	81.18	80.19	64.40	63.57	74.67	73.68	63.08	62.56	41.88	41.38	54.76	53.92	61.52	61.26	43.84	42.29
w/o degree	79.14	80.16	63.49	62.12	74.36	73.28	63.68	62.96	30.89	21.05	32.82	23.07	31.12	21.61	30.44	21.08
ours	82.80	82.49	67.30	66.30	75.88	75.05	66.34	65.70	42.64	41.27	56.36	55.25	62.44	61.66	46.24	44.54

the degree-based prior information to learn expressive node embeddings. Theoretically, we prove that SMILE effectively enhances the model’s generalization performance. Empirically, we conduct extensive experiments on multiple benchmarks and the results suggest that SMILE significantly outperforms other baselines, including both in-domain and cross-domain few-shot settings.

Acknowledgments

Our work is supported by the National Science and Technology Major Project under Grant No. 2021ZD0112500, the National Natural Science Foundation of China (No. 62172187 and No. 62372209). Fausto Giunchiglia’s work is funded by European Union’s Horizon 2020 FET Proactive Project (No. 823783).

References

- [1] Yujia Bao, Menghua Wu, Shiyu Chang, and Regina Barzilay. 2020. Few-shot text classification with distributional signatures. In *ICLR*.
- [2] Peyman Bateni, Raghav Goyal, Vaden Masrani, Frank Wood, and Leonid Sigal. 2020. Improved few-shot visual classification. In *CVPR*.
- [3] Aleksandar Bojchevski and Stephan Günnemann. 2018. Deep gaussian embedding of graphs: Unsupervised inductive learning via ranking. In *ICLR*.
- [4] Kaize Ding, Jianling Wang, Jundong Li, Kai Shu, Chenghao Liu, and Huan Liu. 2020. Graph prototypical networks for few-shot learning on attributed networks. In *CIKM*. 295–304.
- [5] Chelsea Finn, Pieter Abbeel, and Sergey Levine. 2017. Model-agnostic meta-learning for fast adaptation of deep networks. In *ICML*. 1126–1135.
- [6] Chelsea Finn, Aravind Rajeswaran, Sham Kakade, and Sergey Levine. 2019. Online meta-learning. In *ICML*.
- [7] Chelsea Finn, Kelvin Xu, and Sergey Levine. 2018. Probabilistic model-agnostic meta-learning. In *NeurIPS*.
- [8] Sebastian Flennerhag, Andrei A Rusu, Razvan Pascanu, Francesco Visin, Hujun Yin, and Raia Hadsell. 2020. Meta-Learning with Warped Gradient Descent. In *ICLR*.
- [9] Erin Grant, Chelsea Finn, Sergey Levine, Trevor Darrell, and Thomas Griffiths. 2019. Recasting gradient-based meta-learning as hierarchical bayes. In *ICLR*.
- [10] Renchu Guan, Yonghao Liu, Xiaoyue Feng, and Ximing Li. 2021. Paper-publication Prediction with Graph Neural Networks. In *CIKM*.
- [11] Zhichun Guo, Chuxu Zhang, Wenhao Yu, John Herr, Olaf Wiest, Meng Jiang, and Nitesh V. Chawla. 2021. Few-Shot Graph Learning for Molecular Property Prediction. In *The Web Conference*. 2559–2567.
- [12] Bharath Hariharan and Ross Girshick. 2017. Low-shot visual recognition by shrinking and hallucinating features. In *ICCV*. 3018–3027.
- [13] Timothy Hospedales, Antreas Antoniou, Paul Micaelli, and Amos Storkey. 2021. Meta-learning in neural networks: A survey. *IEEE TPAMI* 44, 9 (2021), 5149–5169.
- [14] Kexin Huang and Marinka Zitnik. 2020. Graph meta learning via local subgraphs. In *NeurIPS*. 5862–5874.
- [15] Muhammad Abdullah Jamal and Guo-Jun Qi. 2019. Task agnostic meta-learning for few-shot learning. In *CVPR*. 11719–11727.
- [16] Sungwon Kim, Junseok Lee, Namkyeong Lee, Wonjoong Kim, Seungyoon Choi, and Chanyoung Park. 2023. Task-Equivariant Graph Few-shot Learning. In *SIGKDD*.
- [17] Thomas N Kipf and Max Welling. 2017. Semi-supervised classification with graph convolutional networks. In *ICLR*.
- [18] Seanie Lee, Bruno Andreis, Kenji Kawaguchi, Juho Lee, and Sung Ju Hwang. 2022. Set-based meta-interpolation for few-task meta-learning. In *NeurIPS*. 6775–6788.
- [19] Mengyu Li, Yonghao Liu, Fausto Giunchiglia, Xiaoyue Feng, and Renchu Guan. 2024. Simple-Sampling and Hard-Mixup with Prototypes to Rebalance Contrastive Learning for Text Classification. *arxiv preprint arXiv:2405.11524* (2024).
- [20] Yann Lifchitz, Yannis Avrithis, Sylvaine Picard, and Andrei Bursuc. 2019. Dense classification and implanting for few-shot learning. In *CVPR*.
- [21] Lu Liu, Tianyi Zhou, Guodong Long, Jing Jiang, and Chengqi Zhang. 2019. Learning to propagate for graph meta-learning. In *NeurIPS*.
- [22] Yonghao Liu, Fausto Giunchiglia, Lan Huang, Ximing Li, Xiaoyue Feng, and Renchu Guan. 2025. A Simple Graph Contrastive Learning Framework for Short Text Classification. In *AAAI*.
- [23] Yonghao Liu, Fausto Giunchiglia, Ximing Li, Lan Huang, Xiaoyue Feng, and Renchu Guan. 2025. Enhancing Unsupervised Graph Few-shot Learning via Set Functions and Optimal Transport. In *SIGKDD*.
- [24] Yonghao Liu, Renchu Guan, Fausto Giunchiglia, Yanchun Liang, and Xiaoyue Feng. 2021. Deep attention diffusion graph neural networks for text classification. In *EMNLP*.
- [25] Yonghao Liu, Lan Huang, Bowen Cao, Ximing Li, Fausto Giunchiglia, Xiaoyue Feng, and Renchu Guan. 2024. A Simple but Effective Approach for Unsupervised Few-Shot Graph Classification. In *WWW*.
- [26] Yonghao Liu, Lan Huang, Fausto Giunchiglia, Xiaoyue Feng, and Renchu Guan. 2024. Improved Graph Contrastive Learning for Short Text Classification. In *AAAI*.
- [27] Yonghao Liu, Mengyu Li, Ximing Li, Fausto Giunchiglia, Xiaoyue Feng, and Renchu Guan. 2022. Few-shot node classification on attributed networks with graph meta-learning. In *SIGIR*.
- [28] Yonghao Liu, Mengyu Li, Ximing Li, Lan Huang, Fausto Giunchiglia, Yanchun Liang, Xiaoyue Feng, and Renchu Guan. 2024. Meta-GPS++: Enhancing Graph Meta-Learning with Contrastive Learning and Self-Training. *ACM TKDD* 18, 9 (2024), 1–30.
- [29] Yonghao Liu, Mengyu Li, Di Liang, Ximing Li, Fausto Giunchiglia, Lan Huang, Xiaoyue Feng, and Renchu Guan. 2024. Resolving Word Vagueness with Scenario-guided Adapter for Natural Language Inference. In *IJCAI*.
- [30] Yonghao Liu, Mengyu Li, Wei Pang, Fausto Giunchiglia, Lan Huang, Xiaoyue Feng, and Renchu Guan. 2025. Boosting Short Text Classification with Multi-Source Information Exploration and Dual-Level Contrastive Learning. In *AAAI*.
- [31] Yonghao Liu, Di Liang, Fang Fang, Sirui Wang, Wei Wu, and Rui Jiang. 2023. Time-aware multiway adaptive fusion network for temporal knowledge graph question answering. In *ICASSP*. 1–5.
- [32] Yonghao Liu, Di Liang, Mengyu Li, Fausto Giunchiglia, Ximing Li, Sirui Wang, Wei Wu, Lan Huang, Xiaoyue Feng, and Renchu Guan. 2023. Local and Global: Temporal Question Answering via Information Fusion. In *IJCAI*.
- [33] David J Livingstone. 2000. The characterization of chemical structures using molecular properties. A survey. *Journal of Chemical Information and Computer Sciences* 40, 2 (2000), 195–209.
- [34] Julian McAuley, Rahul Pandey, and Jure Leskovec. 2015. Inferring networks of substitutable and complementary products. In *SIGKDD*. 785–794.
- [35] Nikhil Mishra, Mostafa Rohaninejad, Xi Chen, and Pieter Abbeel. 2018. A simple neural attentive meta-learner. In *ICLR*.
- [36] Subhabrata Mukherjee and Ahmed Awadallah. 2020. Uncertainty-aware self-training for few-shot text classification. In *NeurIPS*. 21199–21212.
- [37] Renkun Ni, Micah Goldblum, Amr Sharaf, Kezhi Kong, and Tom Goldstein. 2021. Data augmentation for meta-learning. In *ICML*. 8152–8161.
- [38] Jaehoon Oh, Hyungjun Yoo, ChangHwan Kim, and Se-Young Yun. 2021. BOIL: Towards Representation Change for Few-shot Learning. In *ICLR*.
- [39] Namyoung Park, Andrey Kan, Xin Luna Dong, Tong Zhao, and Christos Faloutsos. 2019. Estimating Node Importance in Knowledge Graphs Using Graph Neural Networks. In *SIGKDD*. 596–606.
- [40] Janarthanan Rajendran, Alexander Irpan, and Eric Jang. 2020. Meta-learning requires meta-augmentation. In *NeurIPS*. 5705–5715.
- [41] Andrei A Rusu, Dushyant Rao, Jakub Sygnowski, Oriol Vinyals, Razvan Pascanu, Simon Osindero, and Raia Hadsell. 2019. Meta-learning with latent embedding optimization. In *ICLR*.
- [42] Jake Snell, Kevin Swersky, and Richard Zemel. 2017. Prototypical networks for few-shot learning. In *NeurIPS*.
- [43] Zhen Tan, Ruocheng Guo, Kaize Ding, and Huan Liu. 2023. Virtual node tuning for few-shot node classification. In *SIGKDD*.
- [44] Zhen Tan, Song Wang, Kaize Ding, Jundong Li, and Huan Liu. 2022. Transductive Linear Probing: A Novel Framework for Few-Shot Node Classification. In *LoG*. 4–1.
- [45] Jie Tang, Jing Zhang, Limin Yao, Juanzi Li, Li Zhang, and Zhong Su. 2008. Arnetminer: extraction and mining of academic social networks. In *SIGKDD*. 990–998.
- [46] Yonglong Tian, Yue Wang, Dilip Krishnan, Joshua B Tenenbaum, and Phillip Isola. 2020. Rethinking few-shot image classification: a good embedding is all you need?. In *ECCV*. 266–282.
- [47] Oriol Vinyals, Charles Blundell, Timothy Lillicrap, Daan Wierstra, et al. 2016. Matching networks for one shot learning. In *NeurIPS*.
- [48] Jixuan Wang, Kuan-Chieh Wang, Frank Rudzicz, and Michael Brudno. 2021. Grad2task: Improved few-shot text classification using gradients for task representation. In *NeurIPS*.
- [49] Song Wang, Kaize Ding, Chuxu Zhang, Chen Chen, and Jundong Li. 2022. Task-adaptive few-shot node classification. In *SIGKDD*. 1910–1919.
- [50] Song Wang, Yushun Dong, Kaize Ding, Chen Chen, and Jundong Li. 2023. Few-shot node classification with extremely weak supervision. In *WSDM*. 276–284.
- [51] Song Wang, Zhen Tan, Huan Liu, and Jundong Li. 2023. Contrastive Meta-Learning for Few-shot Node Classification. In *SIGKDD*.
- [52] Felix Wu, Amauri Souza, Tianyi Zhang, Christopher Fifty, Tao Yu, and Kilian Weinberger. 2019. Simplifying graph convolutional networks. In *ICML*.
- [53] Xinnuo Xu, Guoyin Wang, Young-Bum Kim, and Sungjin Lee. 2021. AugNLG: Few-shot Natural Language Generation using Self-trained Data Augmentation. In *ACL*.
- [54] Huaxiu Yao, Long-Kai Huang, Linjun Zhang, Ying Wei, Li Tian, James Zou, Junzhou Huang, et al. 2021. Improving generalization in meta-learning via task augmentation. In *ICML*. 11887–11897.
- [55] Huaxiu Yao, Linjun Zhang, and Chelsea Finn. 2022. Meta-learning with fewer tasks through task interpolation. In *ICLR*.
- [56] Mingzhang Yin, George Tucker, Mingyuan Zhou, Sergey Levine, and Chelsea Finn. 2020. Meta-learning without memorization. In *ICLR*.
- [57] Chuxu Zhang, Kaize Ding, Jundong Li, Xiangliang Zhang, Yanfang Ye, Nitesh V Chawla, and Huan Liu. 2022. Few-shot learning on graphs. In *IJCAI*.
- [58] Jian Zhang, Chenglong Zhao, Bingbing Ni, Minghao Xu, and Xiaokang Yang. 2019. Variational Few-Shot Learning. In *ICCV*. 1685–1694.
- [59] Fan Zhou, Chengtai Cao, Kumpeng Zhang, Goce Trajcevski, Ting Zhong, and Ji Geng. 2019. Meta-gnn: On few-shot node classification in graph meta-learning. In *CIKM*. 2357–2360.

Algorithm 1 The process of SMILE

Input: A graph $\mathcal{G} = \{\mathcal{V}, \mathcal{E}, \mathcal{Z}, \mathcal{A}\}$.
Output: The well-trained SMILE.

- 1: // *Meta-training process*
- 2: **while** *not convergence* **do**
- 3: Learn node embeddings using Eq.1.
- 4: Refine node embeddings using Eq.2.
- 5: Construct meta-training tasks \mathcal{D}_{org} .
- 6: Perform within-task mixup to obtain the augmented task \mathcal{T}_t using Eq.3.
- 7: Perform across-task mixup to obtain the interpolated task \mathcal{T}_t^{aug} using Eqs.4 and 5.
- 8: Form the interpolated tasks \mathcal{D}_{aug} .
- 9: Obtain the enriched meta-training tasks \mathcal{D}_{all} .
- 10: Compute the prototypes of support set for each task using Eq.4.
- 11: Optimize the model using Eq.6.
- 12: **end while**
- 13: // *Meta-testing process*
- 14: Construct meta-testing task \mathcal{T}_{tes} .
- 15: Compute the prototypes in \mathcal{S}_{tes} using Eq.7.
- 16: Predict the node labels in \mathcal{Q}_{tes} .

Appendix**A Description of Symbols**

We summarize the used important symbols in Table S1.

Table S1: Descriptions of the symbols.

Symbols	Descriptions
$\mathcal{G}, \mathcal{V}, \mathcal{E}$	Graph, node set, and edge set
\mathcal{Z}, \mathcal{A}	Initialized node features and adjacency matrix
$\hat{\mathcal{D}}, \mathcal{H}, \mathcal{X}$	Degree matrix, hidden vectors, and refined vectors
κ, α, β	Interaction weights, node centralities, and adjusted scores
N, K, M	N way, K shot, M query
\mathcal{D}_{org}	Original meta-training tasks
\mathcal{D}_{aug}	Generated meta-training tasks
\mathcal{D}_{all}	All original and generated meta-training tasks
$\mathcal{S}_t, \mathcal{Q}_t$	Support and query set
n_s, n_q	Number of samples in \mathcal{S}_t and \mathcal{Q}_t
\mathcal{T}_{tes}	Meta-testing task
$\mathcal{S}_{tes}, \mathcal{Q}_{tes}$	Support and query set of \mathcal{T}_{tes}
η, ζ	Hyperparameters in Beta distribution
λ	Random variable drawn from Beta distribution
$\mathcal{S}'_t, \mathcal{Q}'_t$	Generated support and query set
$n_{s'}, n_{q'}$	Number of samples in \mathcal{S}'_t and \mathcal{Q}'_t
m', m	Number of samples in $\mathcal{S}_t \cup \mathcal{S}'_t$ and $\mathcal{Q}_t \cup \mathcal{Q}'_t$
$\mathcal{T}_t^{aug}, \tilde{\mathcal{S}}, \tilde{\mathcal{Q}}$	Interpolated task with its support and query set
T_{org}	Number of tasks in \mathcal{D}_{org}
T_{aug}	Number of tasks in \mathcal{D}_{aug}
T	Number of tasks in \mathcal{D}_{all}

B Training Procedure

We present the training procedure of the proposed SMILE in Algorithm 1.

C Complexity Analysis

We analyze the time complexity of our proposed model to demonstrate its effectiveness. Our model mainly contains two parts, including node presentation learning and dual-level mixup. As linear interpolation is employed in the dual-level mixup, it does not introduce additional time complexity. Basically, most of the time-consuming operations arise from the node embedding process. Here, we choose SGC as the base graph encoder, which removes layer-wise non-linear operations and performs feature extraction in a parameter-free manner. The required time complexity of this step is $O(n^2d)$, where n and d denote the number of nodes and the dimension of node features, respectively. Note that as feature extraction does not require any weights, it is essentially equivalent to a pre-processing step and can be precomputed in practice. Moreover, in the procedure of incorporating degree-based prior information to obtain the refined node representations, the required time complexity is $O(2nd + n)$. Thus, the overall time complexity of our approach is $O(n^2d) + O(2nd + n)$, which is acceptable to us.

D Statistics and Descriptions of Datasets

In this section, we provide detailed statistics and descriptions of the used datasets, which have been widely used in previous studies [4, 27, 49]. The detailed descriptions are provided below.

- **Amazon-Clothing** [34]: It is a product network constructed from the ‘‘Clothing, Shoes, and Jewelry’’ category on Amazon. In this dataset, each product is treated as a node, and its description is used to construct node features. A link is created between products if they are co-viewed. The labels are defined as the low-level product class. For this dataset, we use the 40/17/20 class split for meta-training/meta-validation/meta-testing.

- **Corafull** [3]: It is a prevalent citation network. Each node represents a paper, and an edge is created between two papers if one cites the other. The nodes are labeled based on the topics of the papers. This dataset extends the previously widely used small dataset Cora by extracting raw data from the entire network. For this dataset, we use a 25/20/25 node class split for meta-training/meta-validation/meta-testing.

- **Amazon-Electronics** [34]: It is another Amazon product network that contains products belonging to the ‘‘Electronics’’ category. Each node represents a product, with its features representing the product description. An edge is created between products if there is a co-purchasing relationship. The low-level product categories are used as class labels. For this dataset, we use a 90/37/40 node category split for meta-training/meta-validation/meta-testing.

- **DBLP** [45]: It is a citation network where each node represents a paper, and the edges represent citation relationships between different papers. The abstracts of the papers are used to construct node features. The class labels of the nodes are defined as the publication venues of the papers. For this dataset, we use an 80/27/30 node category split for meta-training/meta-validation/meta-testing.

E Descriptions of Baselines

In this section, we present the detailed descriptions of the selected baselines below.

E.1 Traditional Meta-learning Method

Protonet [42]: It learns a metric space by acquiring prototypes of different categories from the support set and computes the similarity between the query samples and each prototype to predict their categories.

MAML [5]: It enables the meta-trainer to obtain a well-initialized parameter by performing one or more gradient update steps on the model parameters, allowing for rapid adaptation to downstream novel tasks with limited labeled data.

E.2 Meta-learning with Fewer Tasks Method

MetaMix [54]: It enhances meta-training tasks by linearly combining the features and labels of samples from the support and query sets to improve the generalization of the model.

MLTI [55]: It generates additional tasks by randomly sampling a pair of tasks and interpolating their corresponding features and labels, replacing the original tasks for training.

Meta-Inter [18]: It proposes a domain-agnostic task augmentation method that utilizes expressive neural set functions to densify the distribution of meta-training tasks through a bi-level optimization process.

E.3 Graph Meta-learning Method

Meta-GNN [59]: It seamlessly integrates MAML and GNNs in a straightforward manner, leveraging the MAML framework to acquire useful prior knowledge from previous tasks during the process of learning node embeddings, enabling it to rapidly adapt to novel tasks.

GPN [4]: It adopts the concept of Protonet for the few-shot node classification task. It uses a GNN-based encoder and evaluator to learn node embeddings and assess the importance of these nodes, while assigning novel samples to their closest categories.

G-Meta [14]: It constructs an individual subgraph for each node, transmits node-specific information within these subgraphs, and employs meta-gradients to learn transferable knowledge based on the MAML framework.

Meta-GPS [27]: It cleverly introduces prototype-based parameter initialization, scaling, and shifting transformations to better learn transferable meta-knowledge within the MAML framework and adapts to novel tasks more quickly.

X-FNC [50]: It first performs label propagation to obtain rich pseudo-labeled nodes based on Poisson learning, and then filters out irrelevant information through classifying nodes and an information bottleneck-based method to gather meta-knowledge across different meta-tasks with extremely supervised information.

COSMIC [51]: It proposes a contrastive meta-learning framework, which first explicitly aligns node embeddings by contrasting two-step optimization within each episode, and then generates hard node classes through a similarity-sensitive mixing strategy.

TLP [44]: It introduces the concept of transductive linear probing, initially pretraining a graph encoder through graph contrastive learning, and then applying it to obtain node embeddings during the meta-testing phase for downstream tasks.

TEG [16]: It designs a task-equivariant graph few-shot learning framework, leveraging equivariant neural networks to learn adaptive task-specific strategies, aimed at capturing task inductive biases to quickly adapt to unseen tasks.

E.4 Implementation Details of Baselines

For traditional meta-learning models, we follow the same settings as [4, 27], and conduct careful hyperparameter search and report their optimal performance. For meta-learning with fewer tasks models, we uniformly use SGC as the graph encoder. Moreover, we adopt the following additional experimental settings. Specifically, for MetaMix, we allow it to perform task augmentation by generating the same number of nodes as those in the original support and query sets for each meta-training task. For MLTI and Meta-Inter, we make them to generate the same number of additional tasks as in our experiments to ensure fairness. For graph meta-learning baselines, we use the hyperparameters recommended in the original papers. All the experiments are conducted by NVIDIA 3090Ti GPUs with the Python 3.7 and PyTorch 1.13 environment.